

Aptamer-functionalized two-photon SiO₂@GQDs hybrid-based signal amplification strategy for targeted cancer imaging

Huijuan Yan ^{a*}, Shuo Yang ^a, Mengxue Liu ^a, Ke Bao ^b, Wu Ren ^b, Fei Lin ^c, Yiqiao Gao ^a, Zhenghui Wang ^c, Shuanghui Liu ^c, Jieli Lv ^a, Ying Zhao ^{a, d}

^a School of Pharmacy, Xinxiang Medical University, Xinxiang, Henan 453003, P. R. China;

^b School of Medical Engineering, Engineering Technology Research Center of Neuroscience and Control of Henan Province, Xinxiang Engineering Technology Research Center of Intelligent Rehabilitation Equipment, Xinxiang Medical University, Xinxiang, Henan 453003, P. R. China;

^c The First Affiliated Hospital of Xinxiang Medical University, Weihui, Henan 453100, P. R. China;

^d Xinxiang Key Laboratory of Clinical Psychopharmacology, Xinxiang Medical University, Xinxiang, Henan 453003, P. R. China;

^e Department of Pharmacy, Xinxiang First People's Hospital, Xinxiang, Henan 453000, P. R. China.

* Corresponding author. Tel.: +86-373-3831662

E-mail address: yanhujuan2013@126.com (H. J. Yan)

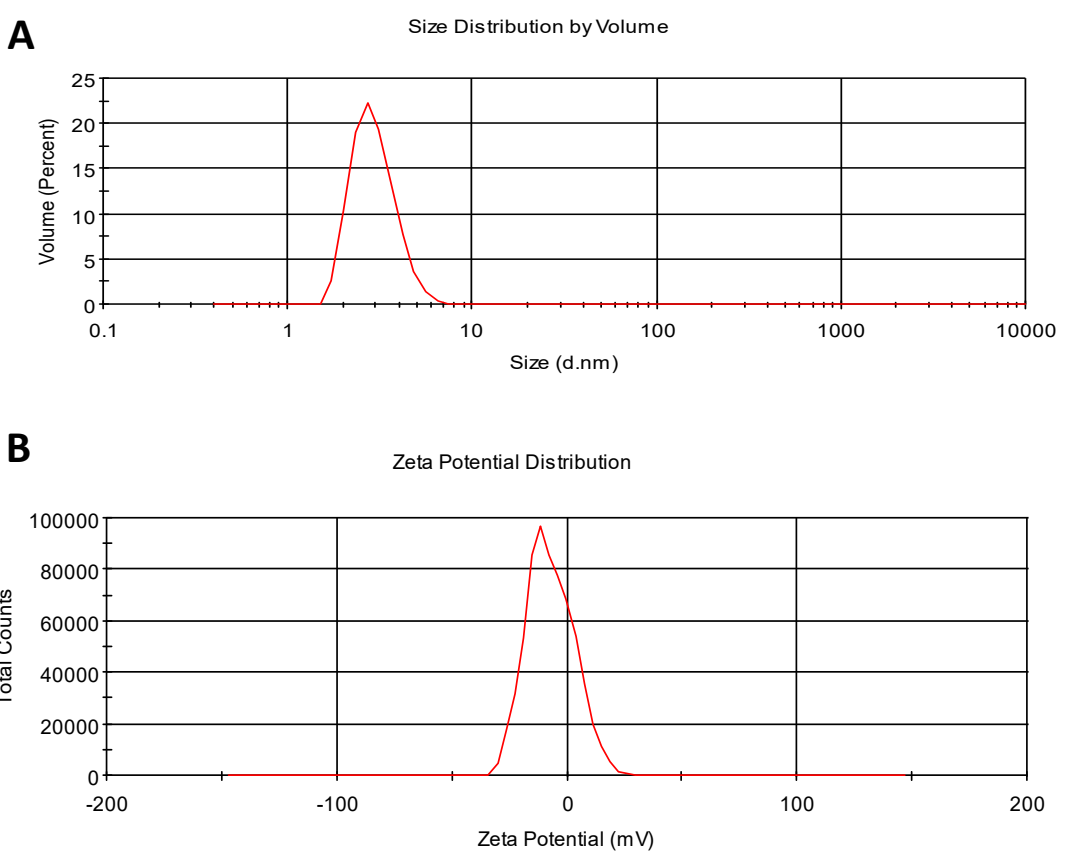


Fig. S1 (A) The DLS and (B) ζ -potential of GQDs.

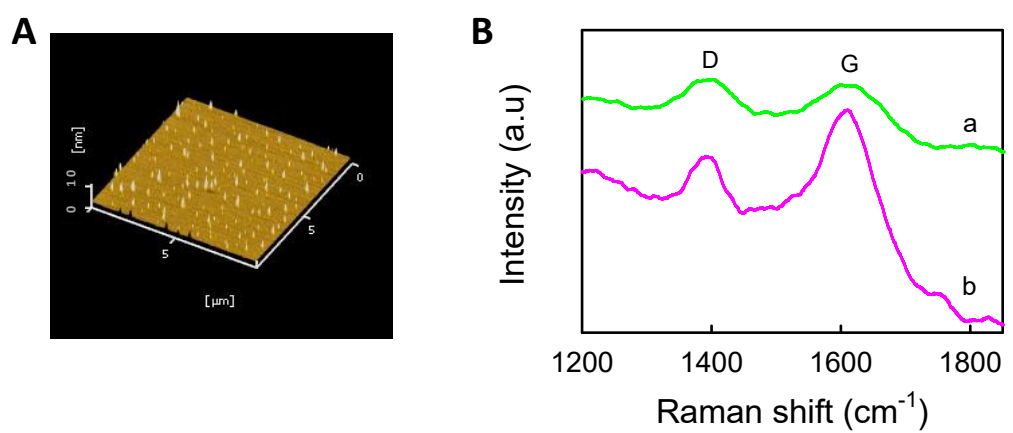


Fig. S2 (A) AFM image of GQDs. (B) The Raman spectra of GO (a) and GQDs (b).

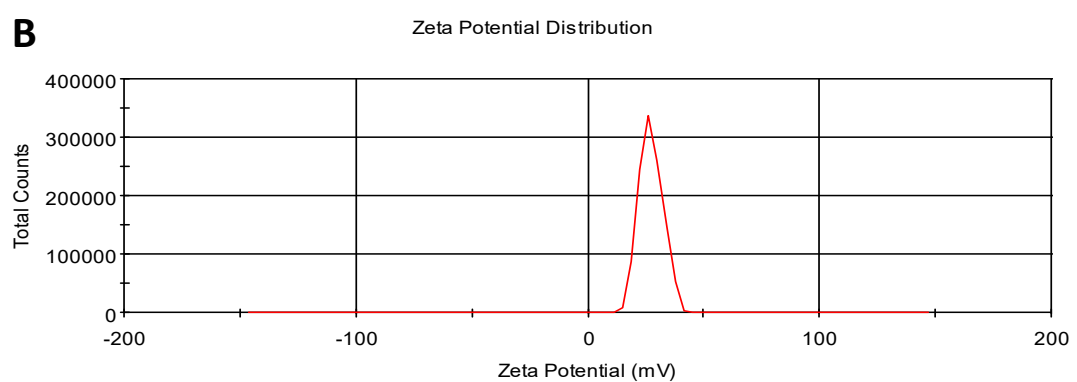
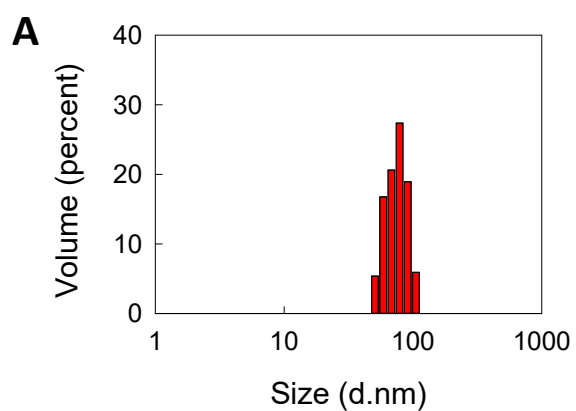


Fig. S3 (A) The DLS and (B) ζ -potential of SiO_2 NPs.

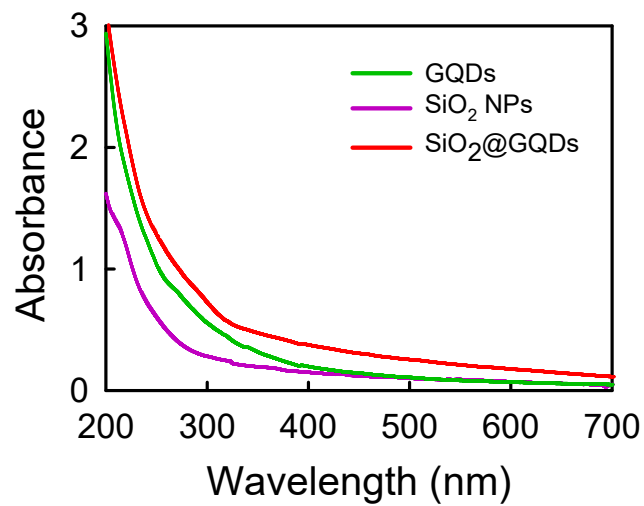


Fig. S4 The UV-vis absorption spectra of aqueous solutions of GQDs, SiO₂ NPs and SiO₂@GQDs.

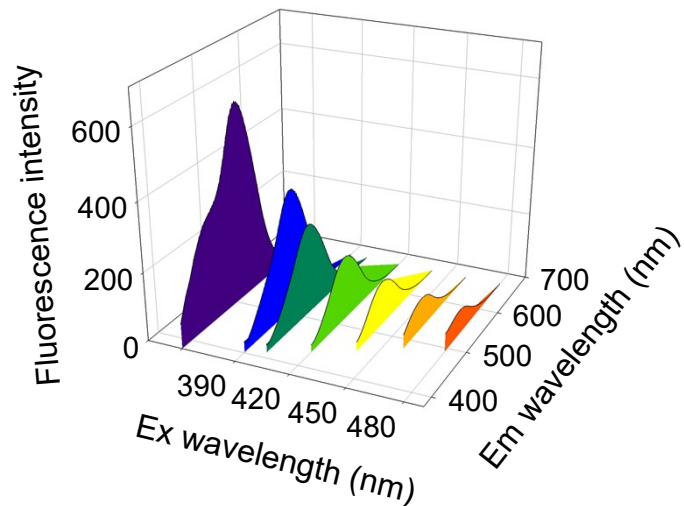


Fig. S5 The effect of different excitation wavelengths on fluorescence emission intensity of GQDs in aqueous solution.

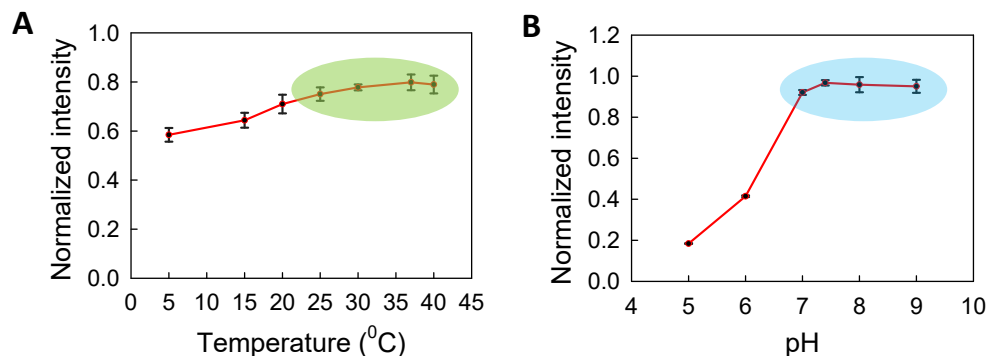


Fig. S6 The effects of temperature (A) and pH (B) on the fluorescence intensity of GQDs in aqueous solution. Ex=390 nm, Em=512 nm.

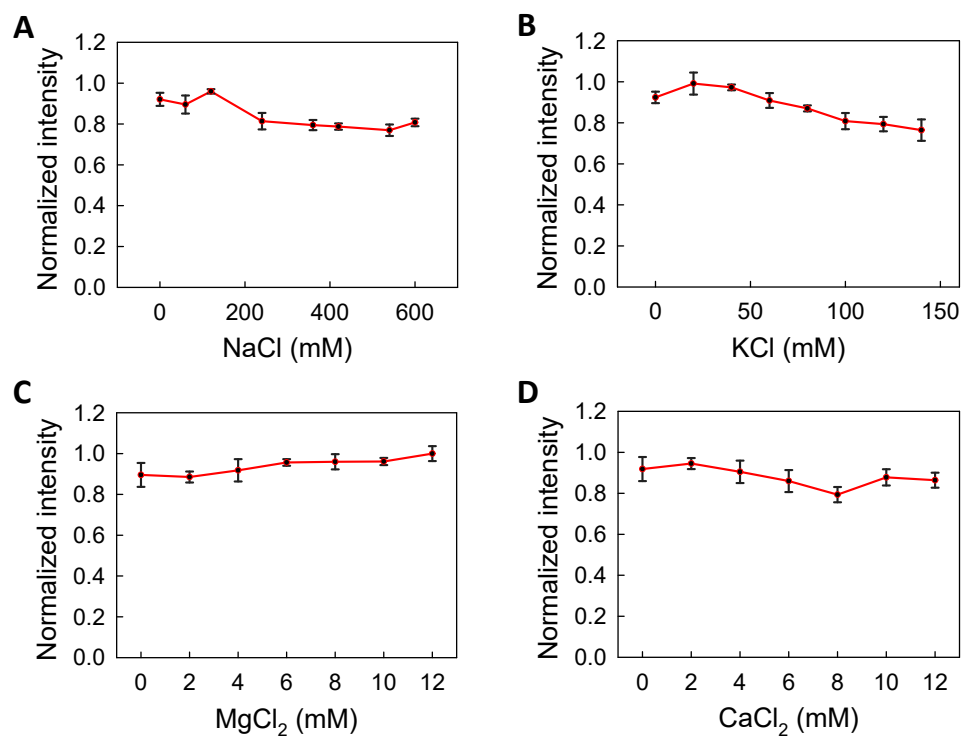


Fig. S7 The effects of different ionic strengths on the fluorescence intensity of GQDs in aqueous solution. Ex=390 nm, Em=512 nm.

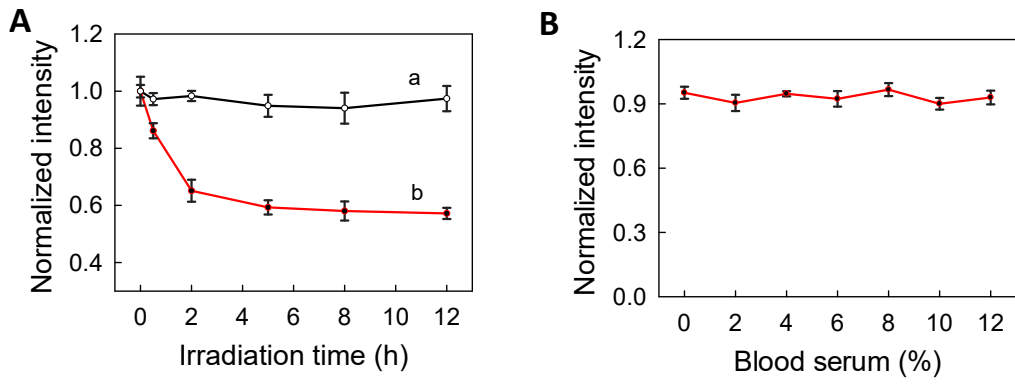


Fig. S8 (A) The effects of temperature (A) and pH (B) on the fluorescence intensity of GQDs in aqueous solution. Ex=390 nm, Em=512 nm. The stability on the fluorescence intensity of GQDs (a) and Rh B (b) in aqueous solution. (B) The stability the fluorescence intensity of GQDs in blood serum-contained solution. Ex=390 nm, Em=512 nm.

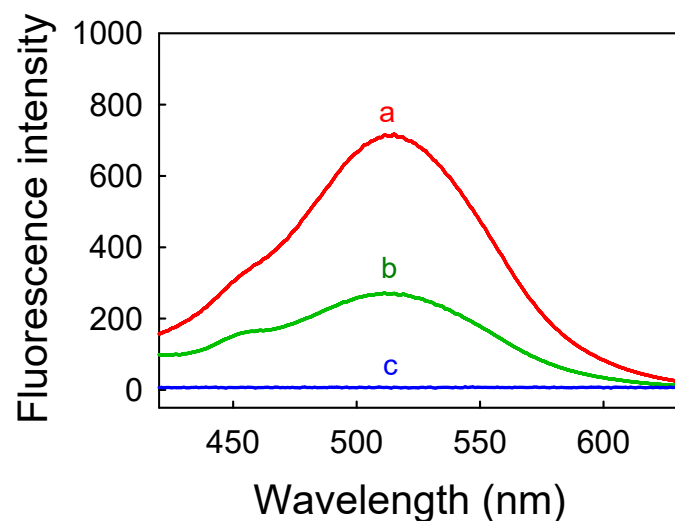


Fig. S9 One-photon intensity of $\text{SiO}_2@\text{GQDs}$ (a), GQDs (b) and SiO_2 NPs (c).

Table S1. Comparison of the fluorescence properties of some GQDs-based nanoprobe

Nanoprobe	Φ (%)	δ (GM)	$\delta \times \Phi$ (GM)	$\lambda_{\text{max, Ex/Em}}$ (nm)	Reference
N-GQDs	28	\	\	370/443	[1]
N-GQDs	34	\	\	360/460	[2]
PLL-GQDs	19.7	\	\	330/454	[3]
GQDs	15.4	\	\	360/450	[4]
N-GQDs	49	\	\	530/533	[5]
GQDs-reflux	0.7	58000	406	800/640	[6]
N, S-GQDs	30	31000	\	800/520	[7]
AuNP-PEP@GQDs	28	\	481	760/516	[8]
TPGQD ⁴²⁰ -BMC3	57.36	\	527	740/420	[9]
SiO ₂ @GQDs	49	\	618	760/512	This work

Notes: Quantum yield (Φ), Two-photon absorption cross-section (δ), Two-photon action absorption cross section ($\delta \times \Phi$), Maximum excitation and emission wavelengths ($\lambda_{\text{max, Ex/Em}}$)

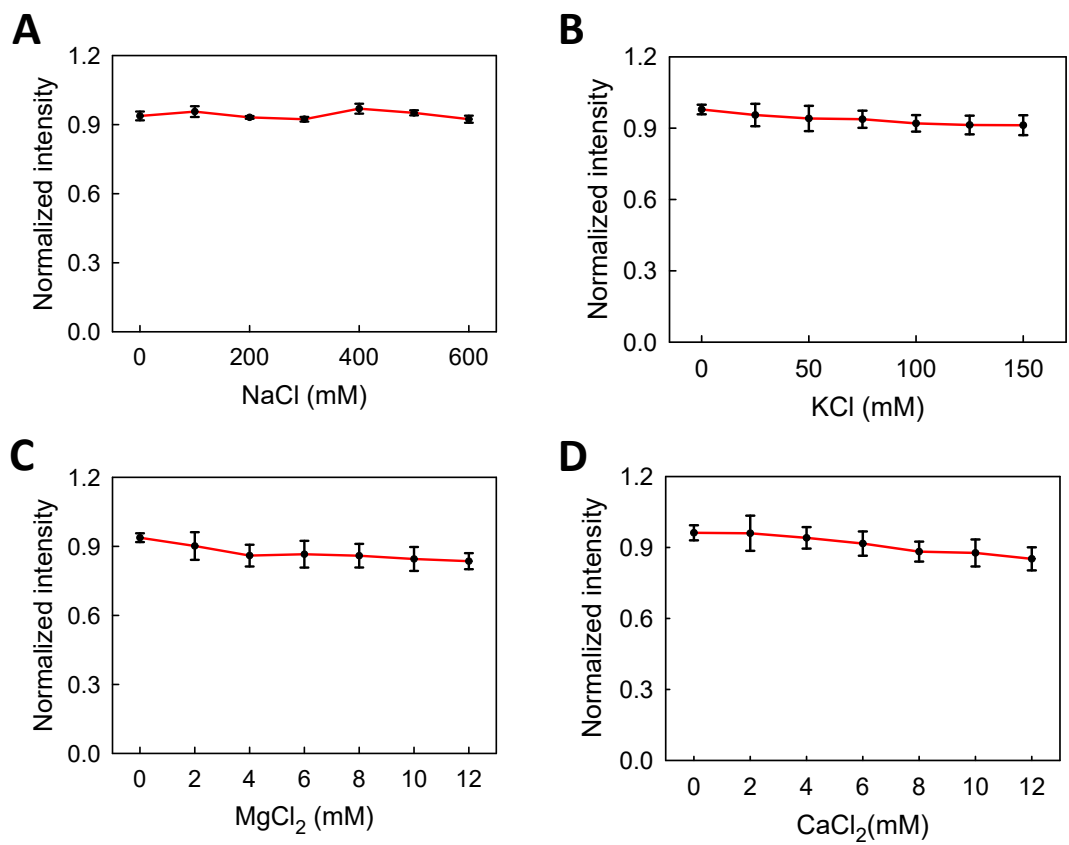


Fig. S10 The effects of different ionic strengths on the fluorescence intensity of SiO₂@GQDs in aqueous solution. Ex=390 nm, Em=512 nm.

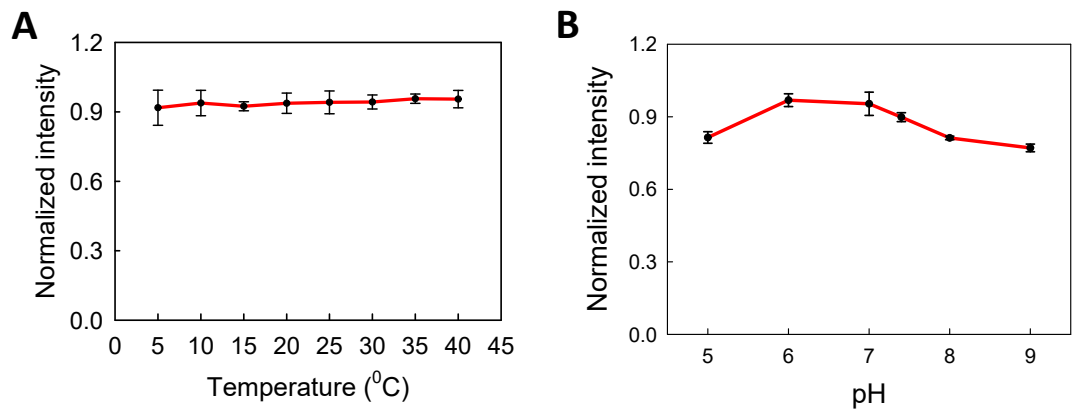


Fig. S11 The effects of temperature (A) and pH value (B) on the fluorescence intensity of $\text{SiO}_2@\text{GQDs}$ in aqueous solution. $\text{Ex}=390\text{ nm}$, $\text{Em}=512\text{ nm}$.

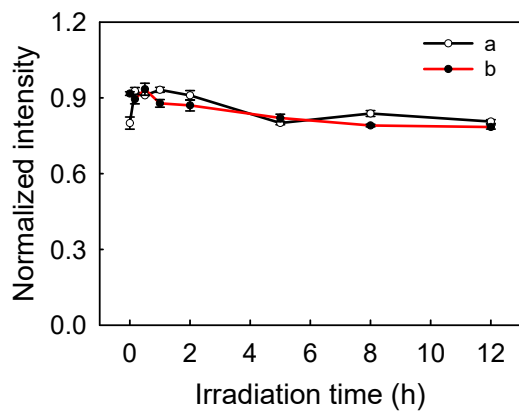


Fig. S12 The stability on the fluorescence intensity of $\text{SiO}_2@\text{GQDs}$ in buffer solution (a) and serum (b). $\text{Ex}=390\text{ nm}$, $\text{Em}=512\text{ nm}$.

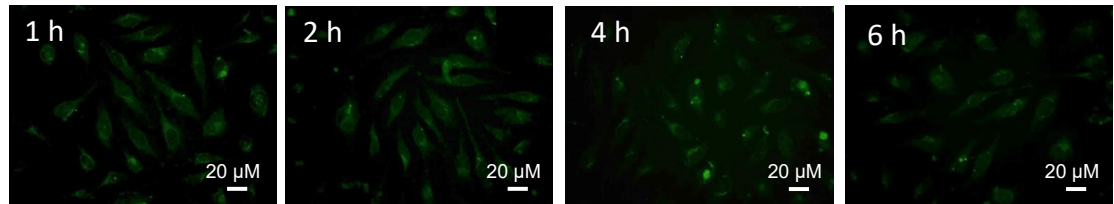


Fig. S13 Confocal microscopy images of the HeLa cells incubated with SiO₂@GQDs for different times.

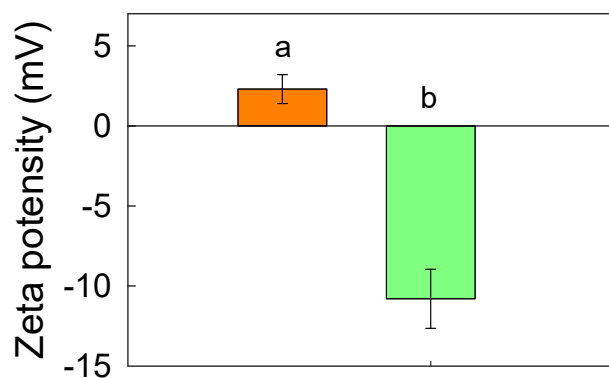


Fig. S14 The ζ -potential of SiO₂@GQDs (a) and SiO₂@GQDs-Sgc8c (b).

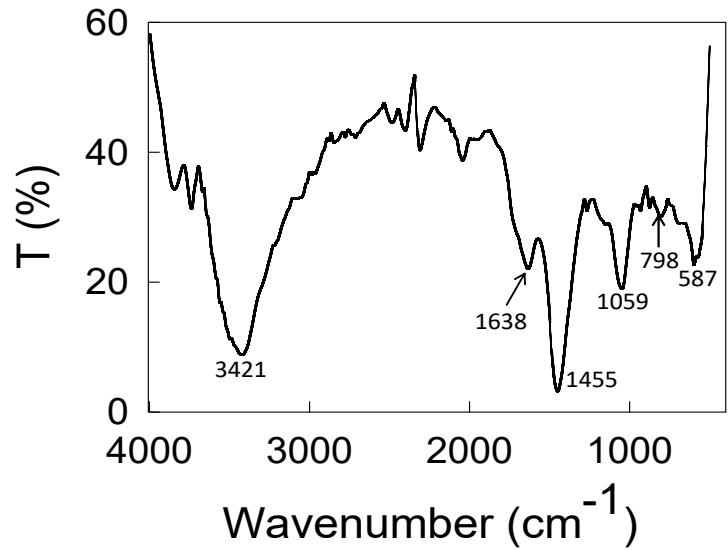


Fig. S15 The IR spectrum of $\text{SiO}_2@\text{GQDs-Sgc8c}$.

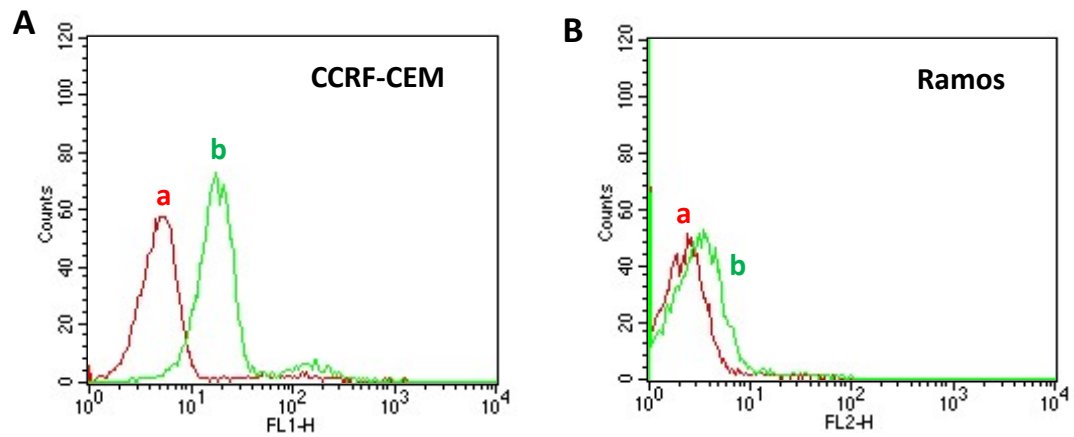


Fig. S16 Flow cytometry assay of CCRF-CEM cells (A) and Ramos cells (B) after incubation with $\text{SiO}_2@\text{GQDs}$ (a) and $\text{SiO}_2@\text{GQDs-Sgc8c}$ (b).

References

- [1] L. L. Zhu, D. B. Li, H. Lu, S. K. Zhang and H. Gao, *Int. J. Biol. Macromol.*, 2022, **194**, 254-263.
- [2] A. B. Ganganboina, A. D. Chowdhury and R. A. Doong, *ACS Appl. Mater. Interfaces.*, 2018, **10**, 614-624.
- [3] R. S. Tade and P. O. Patil, *ACS Biomater Sci Eng.*, 2022, **8**, 470-483.
- [4] Z. Li, Y. Wang, Y. N. Ni and S. Kokot, *Sensor Actuat B-chem.*, 2015, **207**, 490-497.
- [5] N. Pimsin, N. Kongsanan, C. Keawprom, P. Sricharoen, P. Nuengmatcha, W. C. Oh, Y. Areerob, S. Chanhai and N. Limchoowong, *ACS Omega.*, 2021, **6**, 14796-14805.
- [6] B. Yuan, X. M. Sun, J. Yan, Z. Xie, P. Chen and S. Y. Zhou, *Phys.Chem.Chem.Phys.*, 2016, **18**, 25002.
- [7] L. Wang, W. T. Li, M. Li, Q. Q. Su, Z. Li, D. Y. Pan, and M. H. Wu, *ACS Sustainable Chem. Eng.*, 2018, **6**, 4711-4716.
- [8] L. L. Wang, J. Zheng, S. Yang, C. C. Wu, C. H. Liu, Y. Xiao, Y. H. Li, Z. H. Qing, and R. H. Yang, *ACS Appl. Mater. Interfaces.*, 2015, **7**, 19509-19515.
- [9] W. J. Zhao, Y. H. Li, S. Yang, Y. Chen, J. Zheng, C. H. Liu, Z. H. Qing, J. S. Li, and R. H. Yang, *Anal. Chem.*, 2016, **88**, 4833-4840.